

# Study of Overload Effects on Increased Fatigue Life by Meshless Local Petrov-Galerkin Method and Experimental Test

**Ali Moarrefzadeh\***

Department of Mechanical Engineering, Mahshahr Branch,  
Islamic Azad University, Mahshahr, Iran

E-mail: a\_moarrefzadeh@yahoo.com

\*Corresponding author

**Received: 17 September 2024, Revised: 22 January 2025, Accepted: 12 March 2025**

**Abstract:** In this paper, the effect of overload on the fatigue life of the C(T) carbon steel ASTM-A193 samples is investigated. For numerical study, a Meshless Local Petrov-Galerkin (MLPG) method is used to predict fatigue crack propagation for cyclic loading with overload. For this purpose, the effective stress intensity factor (SIF) is introduced as a function depending on cyclic load in the presence of variable amplitude. SIF has been calculated by enriching the weight function. Then, the fatigue crack propagation Equation is calculated with and without overload. In this study, the MLPG method is extended for predicting fatigue crack propagation rate when an overload occurs. The results show the effect of overload delay on the next cycles. Finally, for evaluating this numerical method, experimental methods are applied. The result from the MLPG method has a good agreement with the experimental result.

**Keywords:** Fatigue Crack Propagation, MLPG, Overload, Stress Intensity Factor, Weight Function

**Biographical notes:** Ali Moarrefzadeh received his PhD in Mechanical Engineering from Islamic Azad University in 2019. His current research includes fatigue, fracture mechanics, and computational Mechanics, and also studying overload effects on fatigue crack propagation. He is currently an Assistant Professor at the Department of Mechanical Engineering, Islamic Azad University, Mahshahr, Iran.

Research paper

COPYRIGHTS

© 2025 by the authors. Licensee Islamic Azad University Isfahan Branch. This article is an open access article distributed under the terms and conditions of the Creative Commons Attribution 4.0 International (CC BY 4.0)

<https://creativecommons.org/licenses/by/4.0/>



---

## 1 INTRODUCTION

---

Many engineering structures are displaced under loading with overload. This can lead to the formation of plastic areas at the crack tip. The interference of these plastic areas under different loads will increase or decrease the crack growth rate in the part, which will lead to more accurate fatigue life prediction analyses.

Many experimental tests have been carried out to determine the overload on fatigue crack propagation. Kumar et al. [1] investigated the increase in fatigue life after applying overload and expressed a relationship for the increase in fatigue life in terms of overload ratio. Similar research was done by Borresgo et al. [2] on aluminum alloys. Shuter and Geary [3] showed that the reduction rate of fatigue crack growth depends on the stress intensity factor and stress ratio. Moarrefzadeh et al. [4] modified Walker's Equation to predict the fatigue crack propagation in the presence of overload. The effective stress intensity factor and the effective cycle ratio were defined because of the overload effect. Based on this research, various models have been presented, the most important of which is the Wheeler model [4]. The basis of this model is the change in the size of the plastic area of the crack tip after applying an overload. Another widely used method, which was formed based on Elber's theory [5], is the use of the effective stress intensity factor. In his research, Elber noticed unusual changes in elastic softness in samples under fatigue loading. After Elber, much research was done on crack closure factors; for example, Suresh and Ritchie [6] stated five mechanisms to explain the crack closure phenomenon. Based on their research, when the specimen is loaded, large tensile plastic regions develop near the crack tip, which are often not completely removed with time. As the crack grows into these areas, the plastic area is moved to the crack front, which will reduce the crack driving force. Also, Newman [7] addressed the validation of the crack closure method in predicting fatigue life and methods of measuring this parameter. Harmain [8] presented a model to determine the effect of overload on crack growth and fatigue life. The two main features of Harmain's model are considering the concept of crack closure as a measure of crack growth and relating the effective stress intensity factor after overloading to the effective stress intensity factor in constant amplitude loading.

The finite element method is also used for numerical analysis. In recent decades, the finite element method has shown its ability in various computational fields, and for this reason, it has become one of the most common methods for solving partial differential Equations used by various researchers and specialists. Currently, this method is considered the most common method among the known numerical methods in the

analysis, where the scope of the problem is in the small areas called divided elements, the governing differential Equations of the system are approximated by a set of algebraic Equations for each element. The finite element approach is widely used to determine the stress intensity factor of cracks under complex loadings. Despite the high accuracy and generality of the finite element method, in cases such as elastic-plastic analysis and the study of crack fatigue propagation, which require a large number of stress intensity factor calculations under different loading conditions, these analyses are very time-consuming. Problems related to cracks in arbitrary and complex paths are difficult to solve using the finite element method. Because in this method, the border between the elements is given a default path for crack development, and in order for the border between the elements to match the real path of the crack, the problem must be solved step by step, and at each step, the mesh of elements must be produced again. This increases the amount of calculation error caused by transferring the field solution from the previous elementalization to the new elementalization [9-17]. In recent years, to solve these problems, a new set of computational methods has been presented, which, unlike the finite element method, does not need to mesh the problem area to solve the problem. These methods are called Meshless Local Petrov-Galerkin (MLPG). In this method, only a set of nodes distributed arbitrarily in the problem area is used to construct approximation functions, discretization, and solve partial differential Equations. In general, in this method, there is no need for any predefined elements to approximate the function field [18-19]. Moarrefzadeh et al [19] used MLPG method based on linear elastic fracture mechanics for the prediction of the fatigue crack propagation in the welding residual stress field. They used the MLPG formulation based on the Moving Least Square (MLS) method to interpolate the displacement field due to residual stress and cyclic loading. The results of the prediction based on their research were very close to the experimental results. Singh et al. [20] modified and enriched the MLPG method for solving fracture mechanics problems and introduced this method for modeling fatigue crack propagation. Rao and Rahman [21] introduced the extended meshless method for the construction of linear elastic cracks under single or combined loading conditions. This method includes the new formulation of the MLPG method based on the exact implementation of the boundary and necessary conditions related to the new weight function.

In this paper, the MLPG method for fatigue crack propagation analysis of a plate C(T) is presented. The MLPG formulation based on the MLS method has been used to analyze the cyclic loading with overload. First,

the MLPG method has been used to analyze fatigue crack propagation with cyclic loading. Therefore, the weight function has been enriched to calculate the stress intensity factor. Then, this method to investigate the effect of overload on the fatigue crack propagation rate has been discussed. In this regard, effective stress intensity factor and effective cycle ratio are defined in order to consider overload. Walker's Equation has been modified to predict the fatigue crack propagation rate in the presence of overload. In order to ensure the distance between nodes and the density of nodes, the relationship between the size of the support domain and the squared domain size with the distance between nodes has been discussed. The obtained results clearly show the effect of overload delay on fatigue crack growth caused by compressive residual stress at the crack tip. In order to validate the presented method, the results have been compared with Wheeler's model and experimental test, which shows a good agreement.

## 2 MATERIALS AND SAMPLES

In this research, according to "Fig. 1", the workpiece with C(T) geometry is made of ASTM-A193 carbon steel, whose mechanical properties are shown in "Table1".

**Table 1** Mechanical properties of 2024-T351

E	Yield Stress	Ultimate Tensile Stress	Poisson's Ratio
200 GPa	450 MPa	550 MPa	0.3

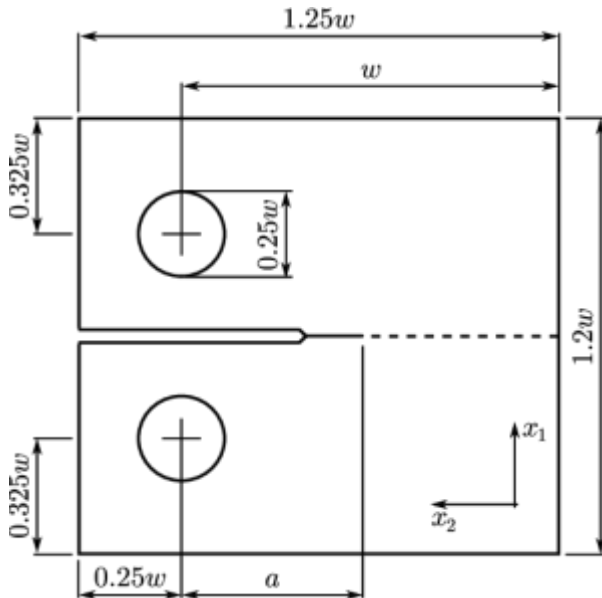


**Fig. 1** Compact Tension (CT) specimen geometry (thickness =3mm).

Figure 2 shows the loading condition of this paper, which is cyclic loading with overload.

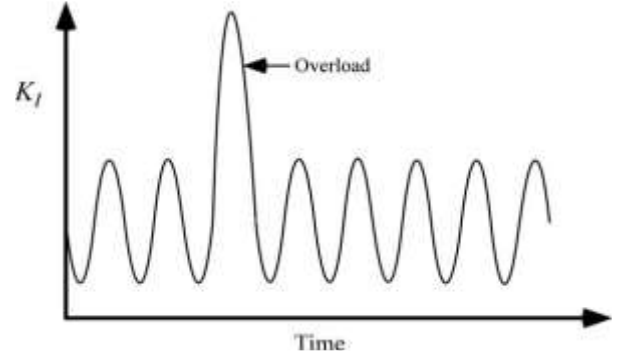


**Fig. 2** Cyclic loading with overload ( $K_I$ :SIF mode 1).

## 3 THEORIES OF MLPG METHOD

The interpolation function according to MLS method is defined [22].

$$U^h(x) = \sum_{i=1}^n \phi_i(x) U_i \quad (1)$$

In this Equation, shape Equation  $\phi_i(x)$ , is given by:

$$\phi_i(x) = \sum_{j=1}^m P_j(x) [A^{-1}(x) B(x)] \quad (2)$$

Where,  $P(x)$  is the basis function:

$$P^T(x) = [1, x, y, x^2, xy, y^2] \quad (3)$$

$A(x)$  and  $B(x)$  are defined as follows:

$$\bar{A}(x) = \sum_{i=1}^n \hat{W}(x - x_i) P(x_i) P^T(x_i) \quad (4)$$

$$B(x) = [w(x - x_1) p(x_1) \dots w(x - x_n) p(x_n)] \quad (5)$$

Also  $W(x - x_i) = W_i$ , the cubic spline weight function is defined according to "Eq. (6)".

$$\hat{W}_i(x) = \begin{cases} \frac{2}{3} - 4r_i^2 + 4r_i^3 & r_i \leq 0.5 \\ \frac{4}{3} - 4r_i + 4r_i^2 - \frac{4}{3}r_i^3 & 0.5 < r_i \leq 1 \\ 0 & r_i > 1 \end{cases} \quad (6)$$

Where,  $r_i$  is the standardized distance between  $x$  and node  $i$ . In solid mechanics, the governing Equation for the two-dimensional problem with residual stress in the domain  $\Omega$  boundary by  $\Gamma$  is described by:

$$\sigma_{ij,j} + d\sigma_{ij,j} = 0 \quad (7)$$

Where  $i, j = (1, 2)$  represent, respectively  $x, y$  directions,  $d\sigma_{ij,j}$  is the residual stress, which is defined as ‘‘Eq. (2)’’.

$$[d\sigma_{residual}] = [D^{ep}]\{d\varepsilon\} \quad (8)$$

Where,  $[D^{ep}]$  is equal to the sum of  $[D^e]$  and  $[D^p]$  which are respectively the elastic stiffness matrix and plastic stiffness matrix. The boundary conditions and initial conditions of the problem are written as follows:

$$\begin{aligned} \sigma_{ij}n_j &= \bar{t}_i \quad \text{on } \Gamma_t \\ u_i &= \bar{u}_i \quad \text{on } \Gamma_u \end{aligned} \quad (9)$$

Where,  $n_j$  is the component of the unit outward normal vector on the boundary and  $\bar{u}_i, \bar{t}_i$  denote the prescribed displacement and tractions, respectively. The local weighted residual form defined over a local quadrature domain  $\Omega_q$  bounded by  $\Gamma_q$ , (shown in ‘‘Fig. 3’’) has the following form.

$$\int_{\Omega_q} \hat{W}_I(\sigma_{ij,j} + d\sigma_{ij,j})d\Omega = 0 \quad (10)$$

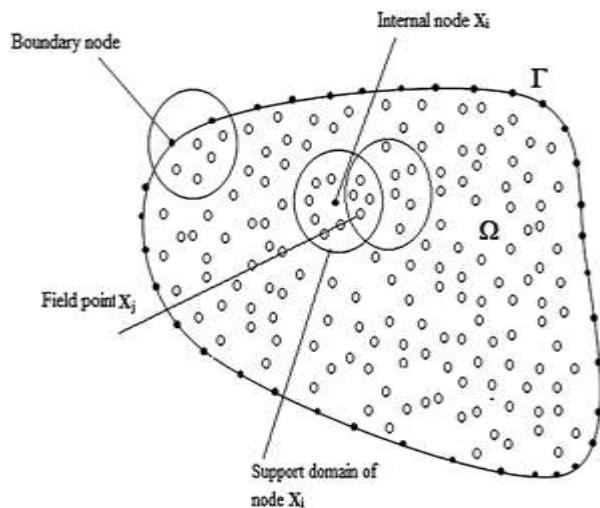


Fig. 3 Support domains of points of interest at  $x_i$  [22].

‘‘Eq. (10)’’ can be integrated by parts to arrive at:

$$\begin{aligned} \int_{\Omega_q} \hat{W}_I(\sigma_{ij,j} + d\sigma_{ij,j})d\Omega &= \\ \int_{\Gamma_q} \hat{W}_I n_j(\sigma_{ij,j} + d\sigma_{ij,j})d\Gamma & \\ - \int_{\Omega_q} \hat{W}_{I,j}(\sigma_{ij,j} + d\sigma_{ij,j})d\Omega &= 0 \end{aligned} \quad (11)$$

Figure 4 shows that the boundary  $\Gamma_q$  for the local quadrature domain,  $\Omega_q$  has been composed by the parts, ie,  $\Gamma_q = \Gamma_{qi} \cup \Gamma_{qt} \cup \Gamma_{qu}$ , where  $\Gamma_{qi}$  is the internal boundary of the quadrature domain, which does not intersect with the global boundary  $\Gamma$ ,  $\Gamma_{qt}$  is the part of the natural boundary that intersects with the quadrature domain and  $\Gamma_{qu}$  is the part of the essential boundary that intersects with the quadrature domain [22]. Therefore, ‘‘Eq. (11)’’ can be rewritten as:

$$\begin{aligned} - \int_{\Omega_q} \hat{W}_{I,j}(\sigma_{ij,j} + d\sigma_{ij,j})d\Omega & \\ + \int_{\Gamma_{qt}} \hat{W}_I(\sigma_{ij,j} + d\sigma_{ij,j})n_j d\Gamma & \\ + \int_{\Gamma_{qu}} \hat{W}_I(\sigma_{ij,j} + d\sigma_{ij,j})n_j d\Gamma & \\ + \int_{\Gamma_{qi}} \hat{W}_I(\sigma_{ij,j} + d\sigma_{ij,j})n_j d\Gamma &= 0 \end{aligned} \quad (12)$$

For a local quadrature domain located entirely within the global domain, there is no intersection between  $\Gamma_q$  and global boundary  $\Gamma$ . Therefore  $\Gamma_{qi} = \Gamma_q$  and there is no integral over  $\Gamma_{qu}$  and  $\Gamma_{qt}$ . In this case, ‘‘Eq. (12)’’ becomes:

$$\begin{aligned} - \int_{\Omega_q} \hat{W}_{I,j}(\sigma_{ij,j} + d\sigma_{ij,j})d\Omega & \\ + \int_{\Gamma_{qi}} \hat{W}_I \sigma_{ij} n_j d\Gamma &= 0 \end{aligned} \quad (13)$$

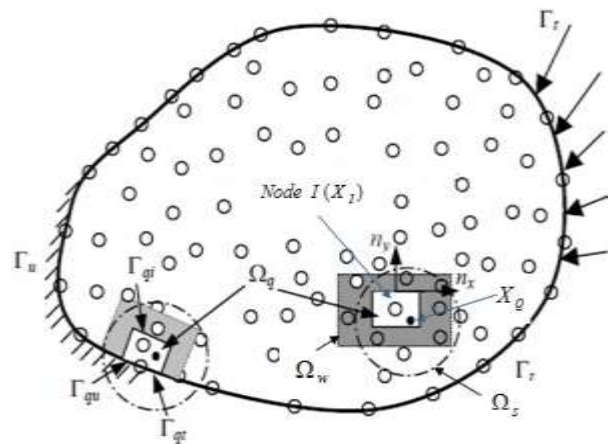


Fig. 4 Schematic illustration of MLPG method [22].

Since the cubic spline weight function has a property that can be zero along the boundary of the internal quadrature domains, the local weak-forms of “Eq. (12)” for nodes whose local quadrature domain intersects with the global boundaries can be rewritten as:

$$\begin{aligned} & - \int_{\Omega_q} \hat{W}_{I,J} (\sigma_{ij,j} + d\sigma_{ij,j_i}) d\Omega \\ & + \int_{\Gamma_{qt}} \hat{W}_I (\sigma_{ij,j} + d\sigma_{ij,j_i}) n_j d\Gamma \\ & + \int_{\Gamma_{qu}} \hat{W}_I (\sigma_{ij,j} + d\sigma_{ij,j_i}) n_j d\Gamma = 0 \end{aligned} \quad (14)$$

By considering this property of the weight function, “Eq. (13)” can be rewritten as:

$$- \int_{\Omega_q} \hat{W}_{I,J} (\sigma_{ij,j} + d\sigma_{ij,j_i})_i d\Omega = 0 \quad (15)$$

By imposing “Eqs. (8) and (9)” in “Eq. (14)”:

$$\begin{aligned} & \int_{\Omega_q} \hat{V}_I^T D^{ep} B d\Omega \\ & - \int_{\Gamma_{qu}} \hat{W}_I^T n D^{ep} B d\Gamma = \\ & \int_{\Omega_q} \hat{V}_I^T \sigma d\Omega + \int_{\Gamma_{qt}} \hat{W}_I^T (\bar{t}_i + d\bar{t}_i) d\Gamma \end{aligned} \quad (16)$$

The “Eq. (16)” can be written in matrix form:

$$K_{IJ} du_j = F_I + G_I \quad (17)$$

In which:

$$K_{IJ} = \int_{\Omega_q} \hat{V}_I^T D^{ep} B d\Omega - \int_{\Gamma_{qu}} \hat{W}_I^T n D^{ep} B d\Gamma \quad (18)$$

$$F_I = \int_{\Gamma_{qt}} \hat{W}_I (\bar{t}_i + d\bar{t}_i) d\Gamma \quad (19)$$

$$G_I = \int_{\Omega_q} \hat{V}_I^T \sigma d\Omega \quad (20)$$

## 4 STRESS INTENSITY FACTOR (SIF)

### 4.1. External Load SIF

One of the most important methods of linear elastic fracture mechanics analysis is the determination of the stress intensity factor. Therefore, calculating the stress intensity factor is very important. Applied load SIF,  $K_{ext}$ , is calculated by:

$$K_{ext} = \sigma_{ext} \sqrt{\pi a} f\left(\frac{a}{W}\right) \quad (21)$$

Where,  $f\left(\frac{a}{W}\right)$  is a specimen geometry dependent function of the crack length,  $a$ , and the specimen width,  $W$ , and  $\sigma_{ext}$  is the applied stress.

### 4.2. Survey of Overload Effect on SIF

Cyclic loading with overload is shown in “Fig. 2”. Overload leads to the formation of a plastic zone in the crack tip. This plastic region is shown in “Fig. 5”.

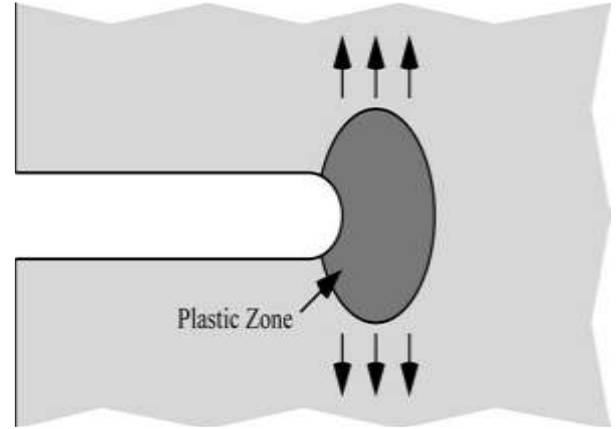


Fig. 5 Plastic zone as a result of overload [24].

But after the overload is lost, due to the lack of coordination between the plastic area of the crack tip and the surrounding elastic environment, a compressive residual stress field according to “Fig. 6” is created around the crack tip. Based on [23], the expression of residual stress  $\sigma_{residual}$  considering elastoplastic hardening in the plastic zone is correspondingly presented:

$$\sigma_{residual} = \int_0^{r_p/w} \Delta\sigma_{res} \cdot F(a, w) \cdot w\left(\frac{x}{w}\right) d\frac{x}{w} \quad (22)$$

Where  $w\left(\frac{x}{a}\right)$  is the weight function depending on the loading, boundary, and geometric condition of the workpiece.

Residual stress SIF  $\Delta K_{residual}$  based on  $\Delta\sigma_{residual}$  is given by the following:

$$\Delta K_{residual} = \sqrt{\pi a} \Delta\sigma_{residual} f\left(\frac{a}{W}\right) \quad (23)$$

Equivalent residual stress SIF  $\Delta K_{residual}^{eq}$  is mainly dependent on load amplitude, which can reflect the

difference between constant and overloaded loading events.

$$\Delta K_{residual}^{eq} = \Delta K_{res}^{constant} + \Delta K_{res}^{overload} - \Delta K_{res}^{overlapping} \quad (24)$$

Where,  $\Delta K_{res}^{constant}$  and  $\Delta K_{res}^{overload}$  are residual stress SIF under constant and overloaded loading, respectively. Also,  $\Delta K_{res}^{overlapping}$  is the overlapping part of  $\Delta K_{res}^{constant}$  and  $\Delta K_{res}^{overload}$ .

In this case, an effective SIF resulting from overload can be defined by:

$$K_{eff(ol)} = K_{ext} - K_{residual}^{eq} \quad (25)$$

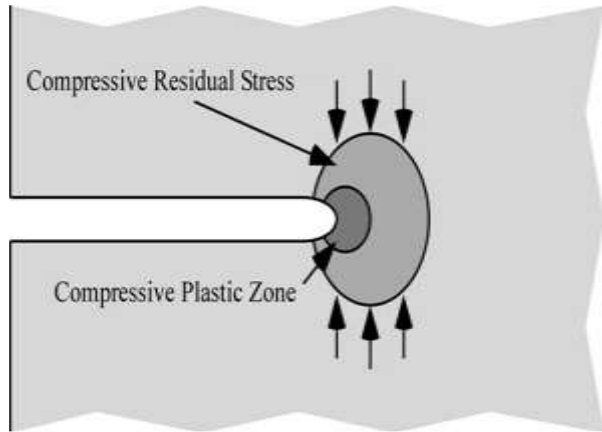


Fig. 6 Residual compressive stresses at crack tip as a result of overload [24].

## 5 FATIGUE CRACK PROPAGATION (FCP)

The stress intensity coefficient and the cycle ratio are very effective for describing the stress field at the crack tip. The fatigue crack propagation rate,  $\frac{da}{dN}$ , is defined

by the stress intensity factor range and cycle ratio. Therefore, the FCP Equation is expressed as a function based on these two parameters.  $(\frac{da}{dN} = f(\Delta K, R))$ .

### 5.1. Survey of Overload Effect on FCP by Wheeler Model

Wheeler introduces a retardation parameter  $\phi$ . It is based on the ratio of the current plastic zone size and the size of the plastic enclave formed at an overload ("Fig. 7").

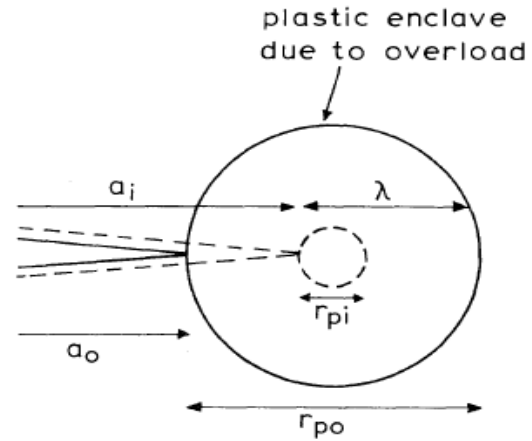


Fig. 7 The model of Wheeler (Situation after overload) [24].

This plastic zone is still embedded in the plastic enclave of the overload; the latter proceeds over a distance  $\lambda$  in front of the current crack  $a_i$ . Wheeler assumes that the retardation factor  $\phi$  will be a power function of  $\frac{r_{pi}}{\lambda}$ .

Since  $\lambda = a_0 + r_{po} - a_i$  the assumption amounts to:

$$\left(\frac{da}{dN}\right)_{retardation} = \phi \left(\frac{da}{dN}\right)_{ordinary} = \phi f(\Delta K) \quad (26)$$

With  $\phi = \left(\frac{r_{pi}}{a_0 + r_{po} - a_i}\right)^m$  as long as

$$a_i + r_{pi} < a_0 + r_{po}.$$

### 5.2. Survey of Overload Effect on FCP by Paris Equation

In order to consider the effect of overload on fatigue crack propagation rate, the Paris Equation is modified as follows:

$$\frac{da}{dN} = c(\Delta K_{ext} - \Delta K_{residual}^{eq})^n \quad (27)$$

### 5.3. Survey of Overload Effect on FCP by Walker Equation

In this case, variation of SIF is defined by Eq. (28). So, considering overload effects, FCP can be obtained by "Eq. (29)". In fact, this Equation is a modification of walker Equation that estimates the rate of FCP considering effects of external loads, overload.

$$\Delta K_{tot} = \Delta K_{eff}^{max} - \Delta K_{eff}^{min} = (K_{ext}^{max} - K_{residual}^{eq}) - (K_{ext}^{min} - K_{residual}^{eq}) = \Delta K_{ext} \quad (28)$$

$$\frac{da}{dN} = c(\Delta K_{ext} (1 - R_{eff}^*)^{m-1})^n \quad (29)$$

Where effective cycle ratio ( $R_{eff}^*$ ) is defined by:

$$R_{eff}^* = \frac{K_{ext}^{min} - K_{residual}^{eq}}{K_{ext}^{max} - K_{residual}^{eq}} \quad (30)$$

Therefore,

$$\frac{da}{dN} = c(\Delta K_{ext} \left( \frac{\Delta K_{ext}}{K_{ext}^{max} - K_{residual}^{eq}} \right)^{m-1})^n \quad (31)$$

Walker Equation has an appealing advantage for predicting FCP rates in compressive residual stress fields due to overload.

#### 5.4. Fatigue Life Estimate Model

In “Eq. (24)”, the effective SIF is introduced. Considering the effect of overload on crack closure, using effective SIF is a suitable method to consider crack growth after overload. For this purpose, “Eqs. (32) and (33)” are expressed for crack growth in this case.

$$\frac{da}{dN} = c_1(\Delta K_{eff})^{n_1} \quad (32)$$

$$\frac{da}{dN} = c_2(\Delta K_{eff}^*)^{n_2} \quad (33)$$

Equations (32) and (33) are used before and after overloading, respectively.

$c_1$  and  $n_1$  are the coefficients related to material properties determined by fatigue testing without overload. Coefficients  $c_2$  and  $n_2$  are obtained by studying “Eq. (33)” on crack growth test data and considering the effect of crack closure. The fatigue life of the workpiece from the initial crack length to the final crack length can be determined by integration in “Eq. (34)”. Since the crack grows discontinuously, this integral turns into a sum and is written:

$$N = \sum_{a_i}^{a_{ol}} \left( \frac{da}{c_1(\Delta K_{eff})^{n_1}} \right) + \sum_{a_{ol}}^{a_f} \left( \frac{da}{c_2(\Delta K_{eff}^*)^{n_2}} \right) \quad (34)$$

In the Linear Elastic Fracture Mechanics (LEFM), the stress field and displacement around the crack mode I are obtained by “Eqs. (35, 36)”:

$$\sigma_{ij} = \frac{K_I}{\sqrt{2\pi r}} f_{ij}(\theta) \quad (35)$$

$$u_i = 2(1+\nu) \frac{K_I}{E} \sqrt{\frac{r}{2\pi}} g_i(\theta) \quad (36)$$

Where,  $r$  is the distance from the crack tip,  $\theta$  is the measured angle relative to the cracks in the counter-clockwise direction,  $K_I$  is Stress Intensity Factor and  $f_{ij}(\theta)$ ,  $g_i(\theta)$  are the standard trigonometric functions of mode I.

The stress intensity factor for external loading,  $K_{ext}$  can be calculated from stresses and displacements:

$$K_I = \frac{u_i}{C\sqrt{r}g_i(\theta)} \quad (37)$$

$$K_I = \sigma_{ij} \frac{\sqrt{2\pi r}}{f_{ij}(\theta)}$$

The distribution of stress and displacement are achieved from the MLPG method according to “Eq. (17)”.

The studied sample is considered according to section 2. According to “Fig. 8”, the stress intensity factor variation is calculated based on the MLPG method with crack propagation for different loading cases. Crack lengths up to 15.3 mm are shown separately in “Fig. 9”. These figures show how the stress intensity factor changes according to the crack propagation.

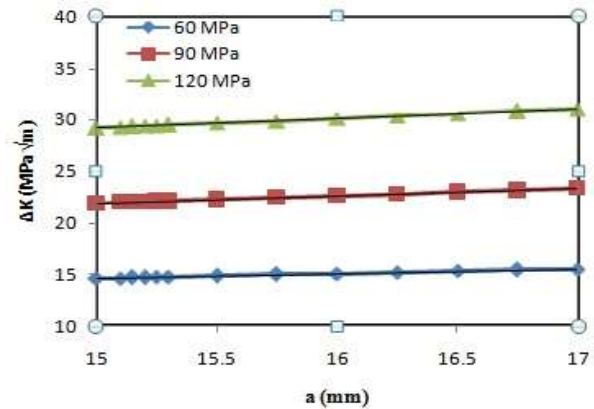


Fig. 8 Stress intensity factor variation (crack length: 15 to 17 mm).

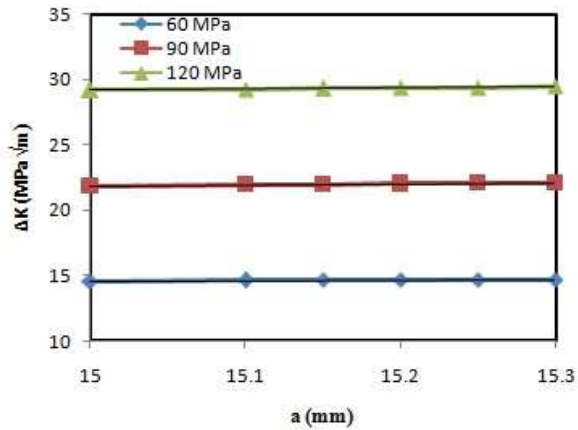


Fig. 9 Stress intensity factor variation (crack length: 15 to 15.3 mm).

According to “Fig. 10”, fatigue crack propagation rates are calculated based on “Eq. (31)” for different loading cases. Crack lengths up to 15.3 mm are shown separately in “Fig. 11”.

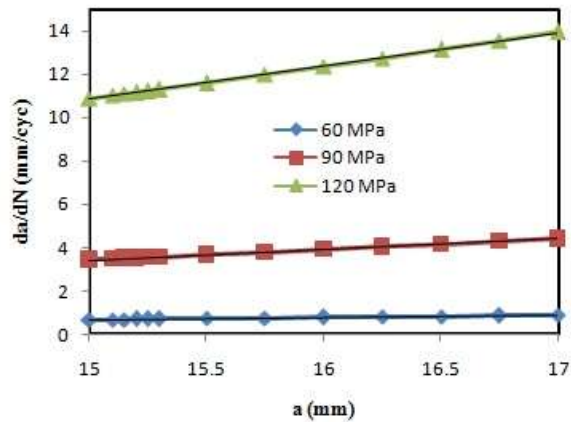


Fig. 10 Fatigue crack propagation rate (crack length: 15 to 17 mm).

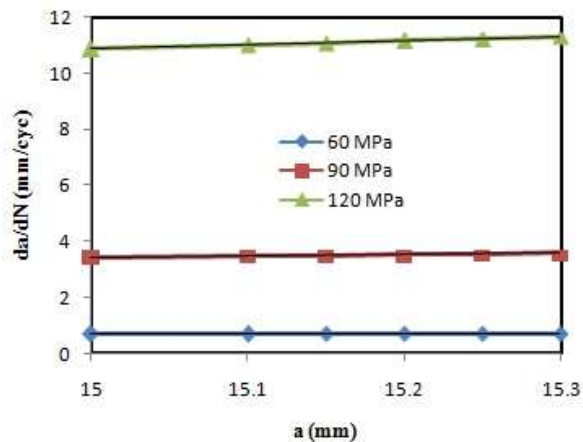


Fig. 11 Fatigue crack propagation rate (crack length: 15 to 15.3 mm).

Variations of external SIF and overload SIF with respect to crack length are shown in “Fig. 12”. The results are obtained based on the MLPG method. In this figure, the effect of overload on the stress intensity factor is shown.

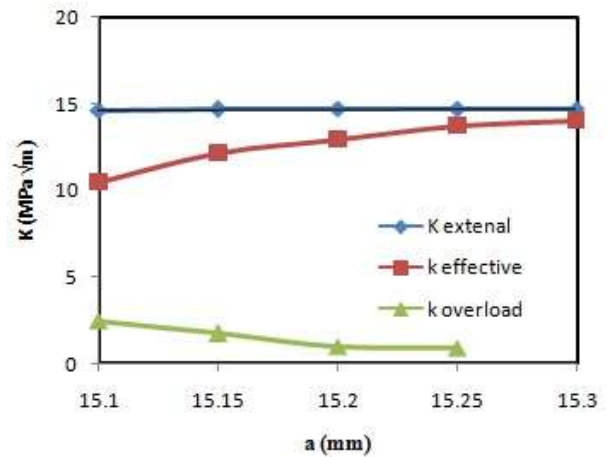


Fig. 12 Effective Stress Intensity Factor (External SIF and overload SIF).

## 7 PREDICTING THE CRACK GROWTH (LOADING WITH VARIABLE AMPLITUDE)

In many structures, the amplitude of cyclic loading is not constant, and the amplitude of the load changes with time. In this research, the expansion of fatigue cracks under load with variable amplitude has been investigated. In this regard, in the case of fatigue crack propagation despite the overload, the mutual effect of loads with different amplitudes has been shown.

In this paper, a large plate made of material according to “Table. 1” and having a geometry according to “Fig. 1” is considered. This plate is under variable tensile stress ( $\Delta\sigma=60MPa$ ). According to MLPG method, fatigue crack propagation rate based on stress intensity factor variation is shown in “Table. 2”.

Table 2 FCP rate based on SIF variation ( $\Delta\sigma=60MPa$ )

da/dN (mm/cyc)	ΔK (MPa√m)
0.679	14.587
0.699	14.708
0.725	14.829
0.744	14.924
0.772	15.066
0.797	15.185
0.821	15.299
0.846	15.412
0.872	15.529

When the crack length is 15 mm, the applied load suddenly doubles. The way of changes in fatigue crack propagation rate in two cases with and without overload is shown in “Fig. 13” based on MLPG method.

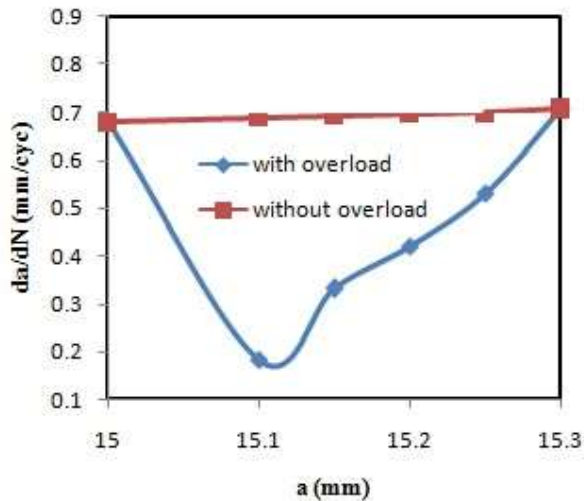


Fig. 13 FCP rate with and without overload.

Figure 14 illustrates this retardation effect of overloads on crack propagation. The overload has introduced a large plastic zone, as shown in “Fig. 5”. The material in this zone is stretched to a permanent deformation, but after unloading, it still has to fit in the surrounding elastic material. The elastic material resumes its original size, but the material in the plastic zone does not. The plastic zone is too large for the surrounding elastic environment.

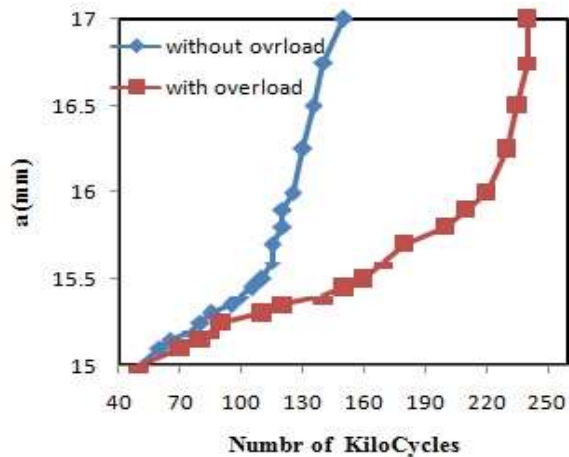


Fig. 14 Delay due to overloading.

Consequently, the surrounding elastic material will exert compressive stresses on the plastically deformed material at the crack tip. The resulting residual stress system is depicted diagrammatically in “Fig. 6”. As soon as the crack has grown through the area of

residual stresses, the original crack propagation curve will resume again.

## 8 DISCUSSIONS

### 8.1. Comparison of the MLPG Method with Experimental Test

Predicted Fatigue crack propagation rates were compared with experimental results for a specimen made of ASTM-A193 carbon steel. The Walker Equation was used to calculate the fatigue crack propagation rates. Material constants used in the walker Equation are  $C = 1.5 \times 10^{-8}$ ,  $n=4$  and  $m=0.5$ .

Figure 15 shows the predicted FCP rates by Walker Equation for  $\Delta\sigma = 60MPa$ . The walker Equation gives a good prediction for this case when  $a \leq 16mm$ . The reason for the difference in results for  $a > 16mm$  is due to the use of LEFM. Fatigue crack propagation test was studied according to ASTM E647 [25].

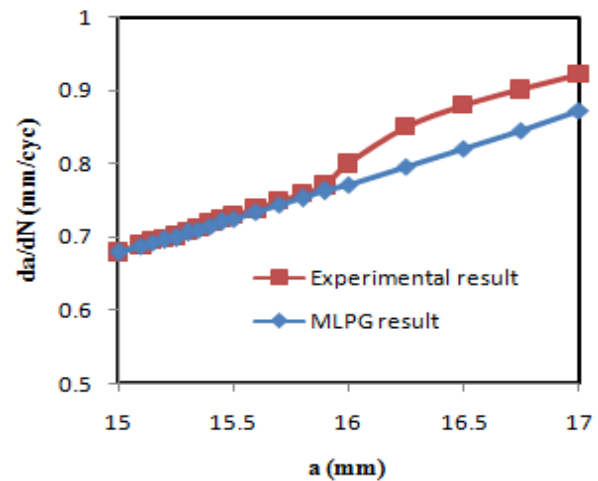


Fig. 15 Comparison of the Walker Equation by experimental test.

### 8.2. Comparison of the MLPG Method with Wheeler's Model

The results of the MLPG method have been compared with the Wheeler model. This comparison is shown in Fig.16. The results show a good agreement. The results obtained based on the two methods are shown up to the crack length of 15.3 mm. Because after this length, the crack comes out of the compressive residual stress area.

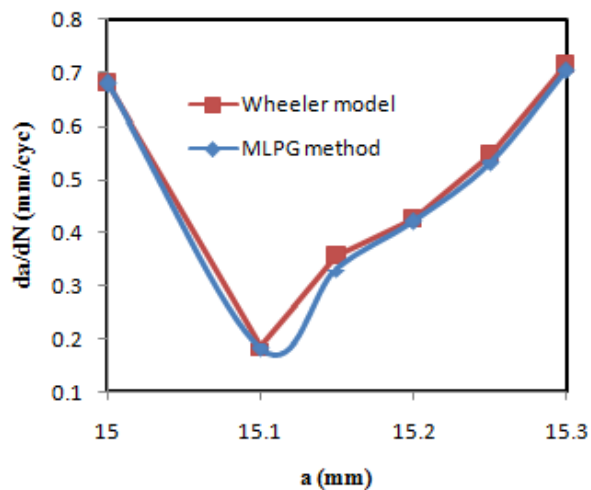


Fig. 16 Comparison of the MLPG method with Wheeler's model.

## 9 CONCLUSIONS

In this paper, the effects of overload on Fatigue crack propagation were studied. The MLPG method is used to calculate the stress intensity factor due to external load and overload. The following results were obtained:

1. By enriching the weight functions to solve crack problems, the stress intensity factor is determined with the desired accuracy, and the number of required nodes is minimized.
2. According to the agreement of the obtained results with the experimental results, it can be said that an efficient method for SIF calculation has been presented.
3. The effects of external load and overload on SIF are considered. Using effective SIF or effective cycle ratio, Walker's Equation is modified to account for the effect of overload on FCP.
4. The agreement of the results of the modified Walker Equation with experimental test and Wheeler model shows that the calculations of overload effects, accomplished according to the MLPG method, are suitable.

## REFERENCES

- [1] Kumar, R., Kumar, A., and Kumar, S., Delay Effect in Fatigue Crack Propagation, *International Journal of Pressure Vessels and Piping*, Vol. 67, No. 1, 1996, pp. 1-5.
- [2] Borresgo, L. P., Ferreira, J. M., Pinho da, J. M., and Cruz, J. M., Evaluation of Overload Effects on Fatigue Crack Growth and Closure, *Engineering, Fracture Mechanics*, Vol. 70, No. 11, 2003, pp. 1379-1397.
- [3] Shuter, D. M., Geary, W., Some Aspects of Fatigue Crack Growth Retardation Behaviour Following Tensile Overloads in A Structural Steel, *Fatigue and Fracture of Engineering Material and Structures*, Vol. 19, No. 10, 1996, pp. 185-199.
- [4] Morrefzadeh, A., Shahrooi, S., and Jalali Azizipour, M., Evaluating the Effects of Overload and Welding Residual Stress in Fatigue Crack Propagation, *Int J Advanced Design and Manufacturing Technology*, Vol. 12, No. 1, 2019, pp. 83-91.
- [5] Elber, W., The Significance of Fatigue Crack Closure, *ASTM STP 486*, 1971.
- [6] Suresh, S., Ritchie, R., Propagation of Short Fatigue Cracks, *International Metallurgical Reviews*, Vol. 29, No. 1, 1984, pp. 445-476.
- [7] Newman, J. C., An Evaluation of Plasticity-Induced Crack Closure Concept and Measurement Methods, *ASTM STP 1343*, 1999, pp. 128-144.
- [8] Harmain, G. A., A Model for Predicting the Retardation Effect Following a Single Overload, *Theoretical and Applied Fracture Mechanics*, Vol. 53, No. 1, 2010, pp. 80-88.
- [9] Sun, J., Pagel, T., and Dilger, K., Generation and Distribution Mechanism of Welding-Induced Residual Stresses, *Journal of Materials Research and Technology*, Vol. 27, 2023, pp. 3936-3954.
- [10] Kollar, D., Volgyi, I., and Joo, A. L., Assessment of Residual Stresses in Welded T-Joints Using Contour Method, *Thin-Walled Structures*, Vol. 190, 2023, pp. 35-48.
- [11] Muzamil M., Akhtar M., Samiuddin, M., and Mehdi, M., Effect of Heat Treatment on Impact Resistance of AU5GT and AS7G06 Aluminum Alloys, *Journal of Mechanical Science and Technology*, Vol. 30, 2016, pp. 4543-4548.
- [12] Spaniel, M., Jurenka, H., and Kuzelka, J., Verification of FE Model of Fatigue Crack Propagation Under Mixed Mode Conditions, *Meccanica*, Vol. 44, 2009, pp. 189-195.
- [13] Ismail, A. E., Ariffin, A. K., Abdullah, S. A., and Ghazali, M. J., Stress Intensity Factors For Surface Cracks in Round Bar Under Single and Combined Loadings, *Meccanica*, Vol. 47, 2012, pp. 1141-1156.
- [14] Wu, X., Carlsson, J., Welding Residual Stress Intensity Factors for Half-Elliptical Surface Cracks in thin and Thick Plates, *Engineering Fracture Mechanics*, 1984, pp. 407-426.
- [15] Itoh Y., Suruga C., Prediction of Fatigue Crack Growth Rate in Welding Residual Stress Fields, *Engineering Fracture Mechanics*, Vol. 33, 1989, pp. 397-407.
- [16] Teng, L., Lin, C. H., Effect of Welding Conditions on Residual Stresses Due to Butt Welds, *International Journal of Pressure Vessels and Piping*, Vol. 75, 1998, pp. 857-864.
- [17] Bao, R., Xiang, Z., and Norvahida, A., Evaluating Stress Intensity Factors Due To Weld Residual Stresses by The Weight Function and Finite Element Methods, *Engineering Fracture Mechanics*, Vol. 7, 2010, pp. 2550-2566.
- [18] Sladek, J., Stanak, P., Tlan, D. Z., Sladek, V., and Atluri, S. N., Applications of the MLPG Method in Engineering and Science: A Review, *Computer Modeling in Engineering and Sciences*, Vol. 92, 2013, pp. 423-475.

- [19] Moarrefzadeh, A., Shahrooi, S., and Jalali Azizpour, M., Predicting Fatigue Crack Propagation in Residual Stress Field Due To Welding by Meshless Local Petrov-Galerkin Method, *Journal of Manufacturing Processes*, Vol. 45, 2019, pp. 379-391.
- [20] Singh, I., Mishra, B., and Pant, M., A Modified Intrinsic Enriched Element Free Galerkin Method for Multiple Cracks Simulation, *Materials & Design*, Vol. 31, 2010, pp. 628-632.
- [21] Rao, B., Rahman, S., A Coupled Meshless Finite Element Method for Fracture Analysis of Cracks, *International Journal of Pressure Vessels and Piping*, Vol. 78, 2001, pp. 647-657.
- [22] Liu, G. R., Gu, Y. T., *An Introduction to Meshfree Methods and Their Programming*, Publisher Springer, 2005.
- [23] Wu, X. R., Carlsson, A. J., *Weight Functions and Stress Intensity Factor Solutions*, Oxford, 1991.
- [24] Broek, D., *Elementary Engineering Fracture Mechanics*, Kluwer Academic Publishers Group, 1982.
- [25] ASTM Standard E647-05, *Standard Test Method for Measurement of Fatigue Crack Growth Rates*, Annual Book of ASTM Standards, 1998, ASTM International, West Conshohoken, PA.